# Supplementary Information

Jackson et al. **Molecular basis for the production of cyclic peptides by plant asparaginyl endopeptidases**

**a**

| Character | Violaceae | Fabaceae | Cucurbitaceae | Rubiaceae | Solanaceae |
|---|---|---|---|---|---|
| Gene origin | Specific | Albumin | Specific | Specific | Specific |
| N-term domains | Multi/Singletons | None | Multi | Multi/Singletons | Singleton |
| Cyclotide domains | Multi/Singletons | Singleton | Multi | Multi/Singletons | Singleton |
| Topologies present | Bracelet/Möbius/Hybrid | Bracelet/Möbius/Hybrid | Squash-TI | Bracelet/Möbius/Hybrid | Bracelet |

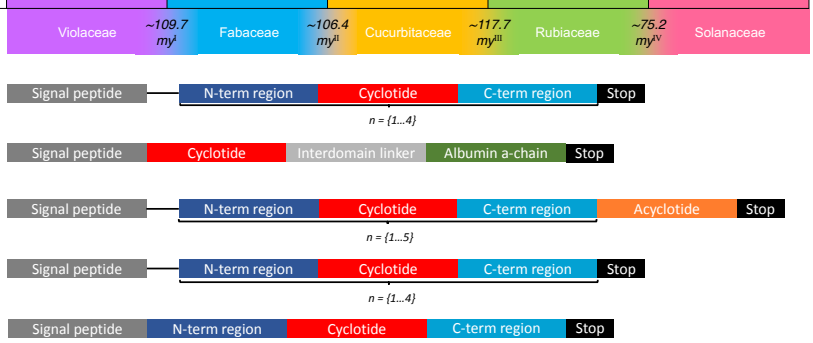


I. Divergence of Malpighiales; II. Most recent common ancestor between Rosales – (Cucurbitales + Fagales);
III. Divergence of Saxifragales; IV. Most recent common ancestor between Gentianales - Solanales

**b**

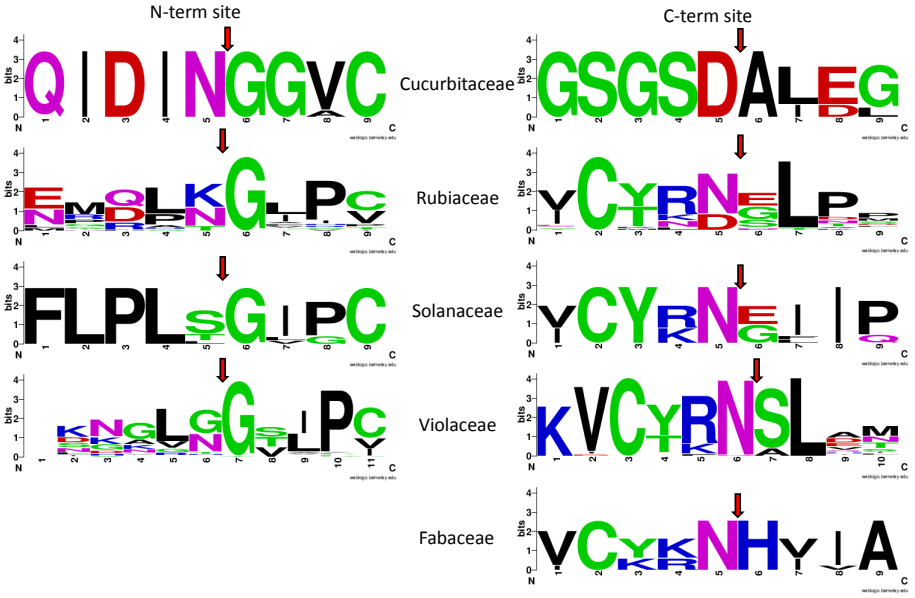


**Supplementary Figure 1. Summary of cyclotide-encoding gene diversity. a,** Attributes of cyclotide precursors and domains across five plant families. All cyclotide encoding genes discovered in the Violaceae, Cucurbitaceae, Rubiaceae, and Solanaceae exist as dedicated expression units, whereas in the Fabaceae, cyclotides are encoded within an albumin gene[1,2]. All precursors possess a signal peptide that directs biosynthesis of cyclotides into the plant cells endomembrane system. Cleavage at the amino terminus of the cyclotide domain must occur first in order to free up the N-terminus for an AEP mediated transpeptidation reaction with the C-terminus of the nascent cyclotide. With the exception of cyclotides in the Solanaceae and Fabaceae, cyclotides domains are often encoded as repeated units. Mature cyclotides are classified into either the Möbius, bracelet or trypsin inhibitor like sub families, where the Möbius and bracelets are characterised by the presence or absence of a twist in the backbone respectively[3], with the trypsin inhibitor class categorised by function. Estimates of evolutionary time between cyclotide producing clades as provided by [4]. For Malpighiales (contains Violaceae) and Saxifragales (contains Fabaceae), divergence time estimates are for that order. Most recent common ancestor estimates are for the last common ancestor of II Fabaceae and Curcubitaceae, and IV Rubiaceae and Solanaceae. **b,** N- and C-terminal precursor sequence diversity across cyclotide-producing plant families. N-terminal processing sites are diverse, with flanking residues suggesting cleavage by AEPs or enzymes with trypsin-like activity. In the Fabaceae, the N-terminus is cleaved by a signal peptidase during translation into the ER thus no N-terminal logo is given. At the C-terminus, an Asx residue is required for transpeptidation by AEP. Other residues appear conserved before the Asx residue (ex: Tyr, Arg, Lys), and after the Asx (ex. Gly).

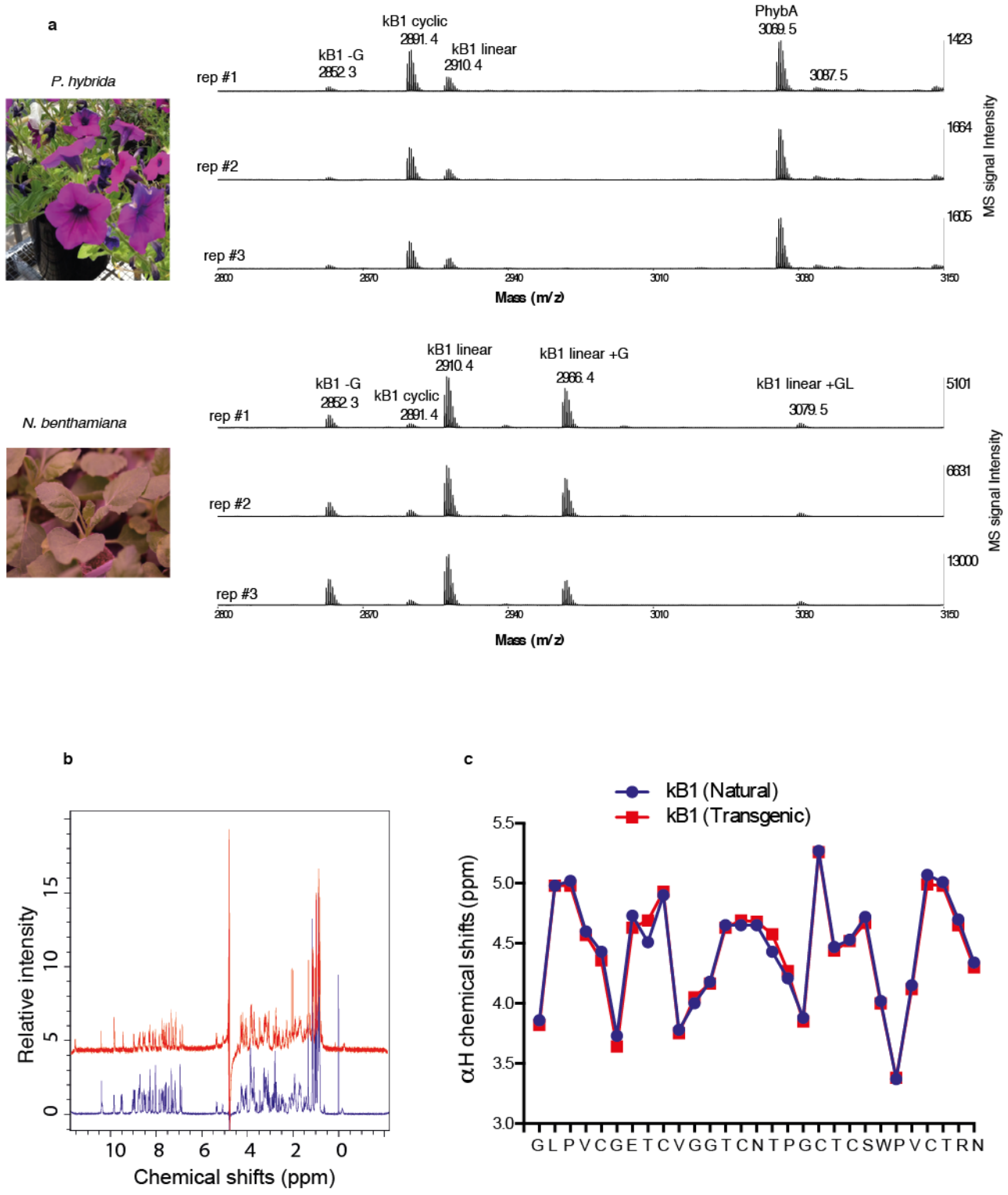


**Supplementary Figure 2. Petunia correctly processes *Oak1* into predominant cyclic kB1. a**, MALDI-MS analysis of petunia and *N. benthamiana* produced peptides upon expression of *Oak1*. Predominant peptide mass signals for cyclic kB1 (2891.4 m/z) are evident in petunia leaf extracts whilst predominant linear kB1 related peptides (2910.4, 2966.4, 3079.5 m/z) are evident in *N. benthamiana* leaf extracts. The peptide mass of 3069.5 m/z in petunia leaf extracts represents the endogenous cyclotide PhybA[5]. **b**, Comparative NMR analysis of *oak1* transgene derived kB1 extracted from petunia with kB1 extracted from *O. affinis* plants. Purified kB1 from petunia leaf (in red) has an identical (b) 1D NMR spectra and (c) αH chemical shifts to that of native kB1 from *O. affinis* (in blue).

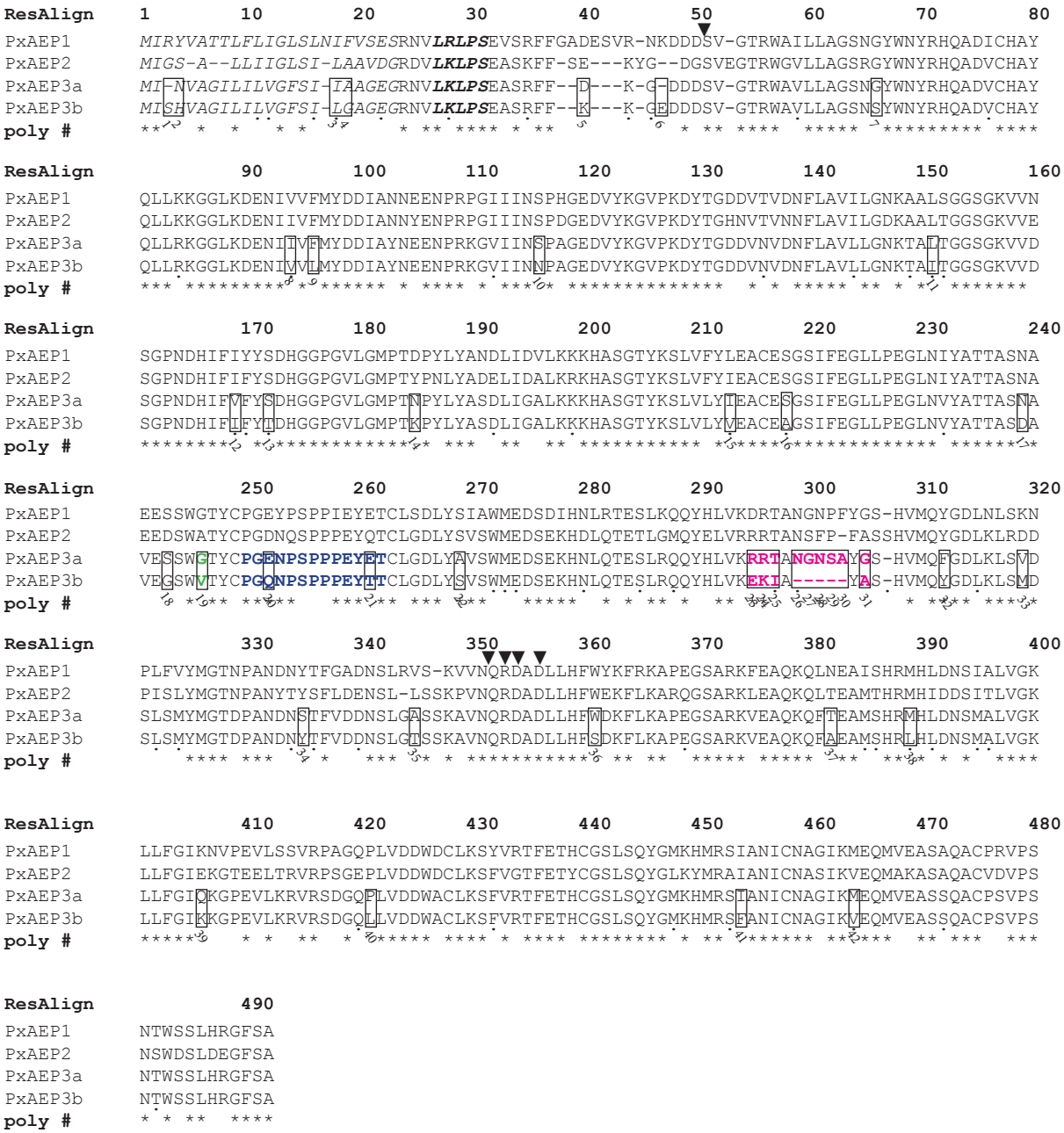

**Supplementary Figure 3. Alignment of petunia AEP isoforms.** Protein sequences were aligned using ClustalW[6]. Identical residues are marked with a star and similar residues with a dot. Putative signal peptides predicted by SignalP 4.0[7] are italicized with putative propeptide cleavage sites indicated by arrows and proposed based on[8]. Boxed residues indicate putative N-terminal vacuole targeting signals as predicted by[9]. The catalytic histidine and cysteine residues are highlighted in yellow. The residue homologous to the Gatekeeper residue of OaAEP1$_b$[8] is shown in green with the cysteine flanking poly-proline loop in blue. The marker of ligase activity (MLA) (this study) is shown in magenta. All polymorphic residues between PxAEP3a and PxAEP3b are underlined.

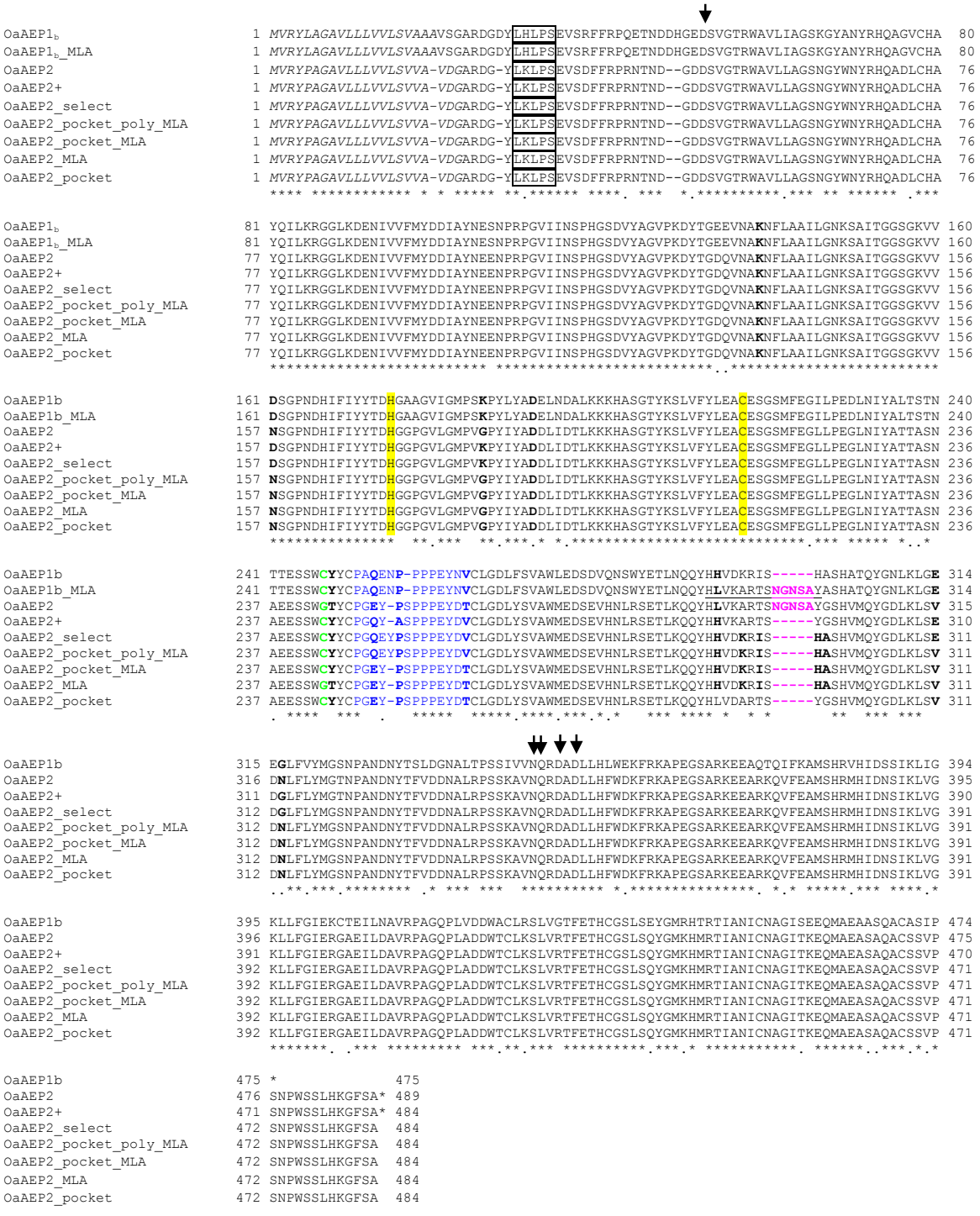


**Supplementary Figure 4. Alignment of *O. affinis* AEP isoforms and engineered variants.** Protein sequences were aligned using ClustalW[6]. Identical residues are marked with a star and similar residues with a dot. Putative signal peptides predicted by SignalP 4.0[7] are italicized with putative propeptide cleavage sites indicated by arrows and proposed based on [8]. Italicized and bolded residues indicate putative N-terminal vacuole targeting signals as predicted by bioinformatics analysis[9]. Boxed are residues that are polymorphic between AEP isoforms PxAEP3a and PxAEP3b. The catalytic histidine and cysteine residues are highlighted in yellow. The gatekeeper residue of OaAEP1$_b$[8] is shown in green with the cysteine flanking poly-proline loop in blue. The marker of ligase activity (MLA) (this study) is shown in magenta. The residues in bold are at positions predicted to be important for AEP ligase function by the protein space modelling.

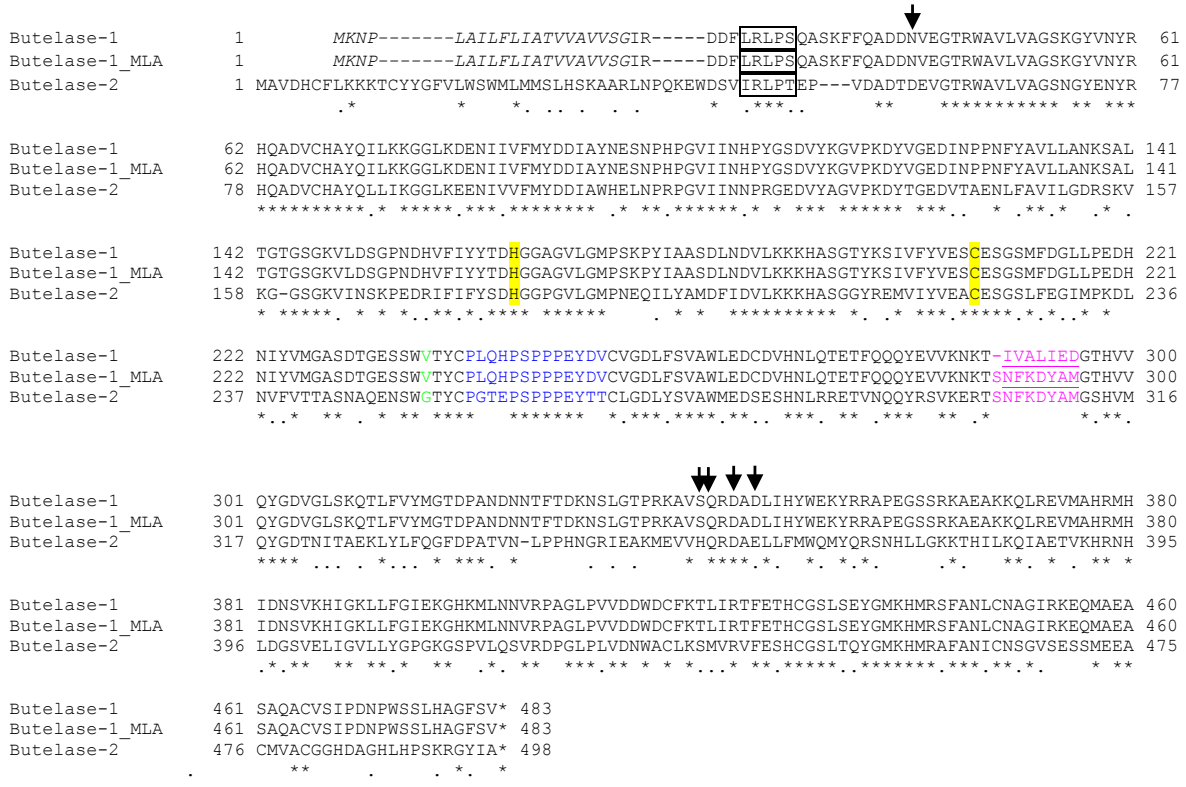


**Supplementary Figure 5. Alignment of *C. ternatea* AEP isoforms and engineered variants.** Protein sequences were aligned using ClustalW[6]. Identical residues are marked with a star and similar residues with a dot. Putative signal peptides predicted by SignalP 4.0[7] are italicized with putative propeptide cleavage sites indicated by arrows and proposed based on[8]. Boxed residues indicate putative N-terminal vacuole targeting signals as predicted by[9]. The catalytic histidine and cysteine residues are highlighted in yellow. The residue homologous to the gatekeeper residue of OaAEP1$_b$[8] is shown in green with the cysteine flanking poly-proline loop in blue. The marker of ligase activity (MLA) (this study) is shown in magenta.

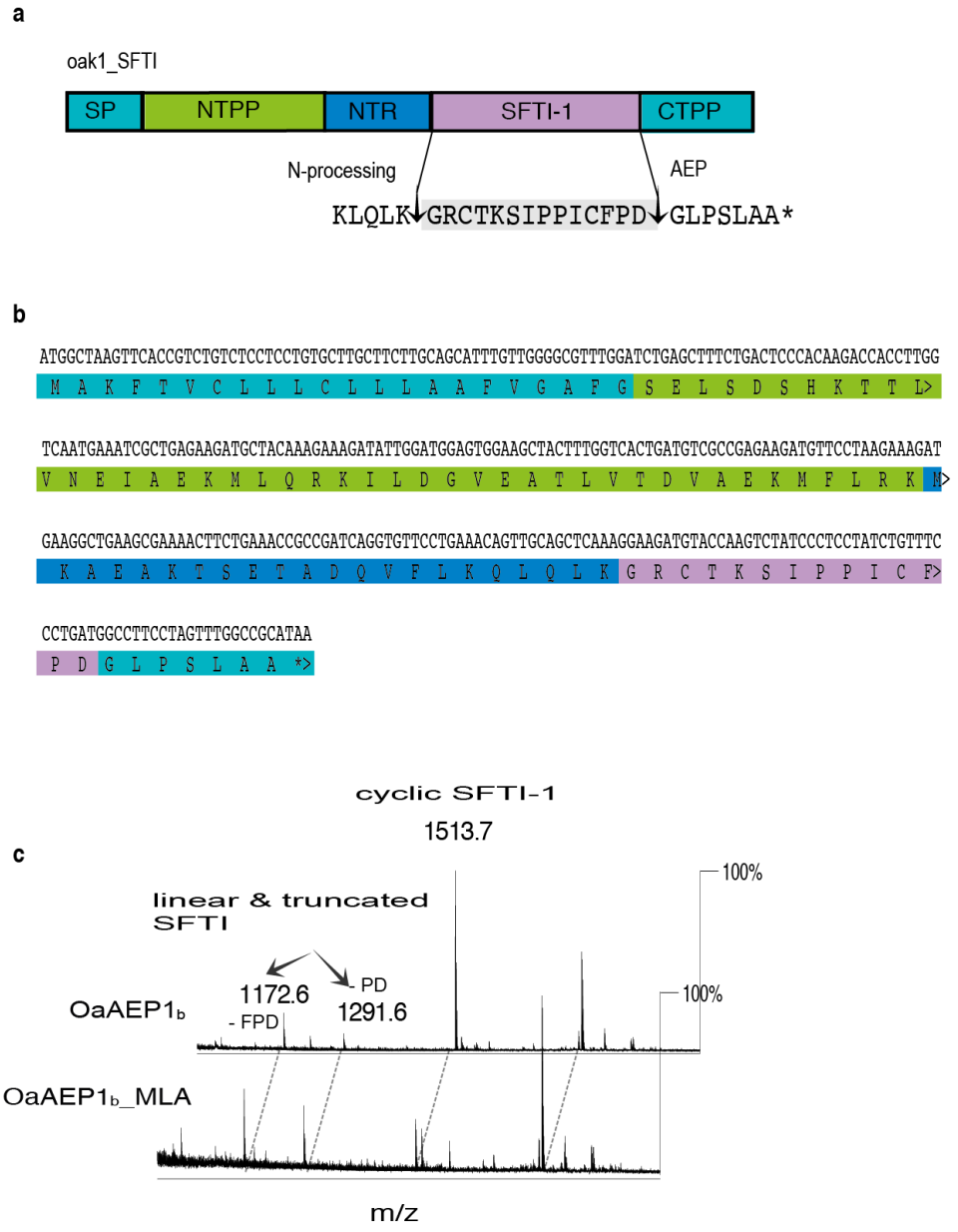


**Supplementary Figure 6. AEP mediated SFTI-1 cyclisation in *N benthamiana* leaves. a,** Schematic of the *Oak1* precursor gene modified to encode the SFTI peptide in replace of kB1. **b,** DNA and protein sequence of *Oak1-SFTI*. **c,** Representative MALDI-MS of peptides produced in *N. benthamiana* leaf upon co-expression of *Oak1-SFTI* with OaAEP1$_b$ and OaAEP1$_b$_MLA. Cyclic SFTI was readily detected in the case of OaAEP1$_b$ but not with OaAEP1$_b$_MLA. In either case no linear full length SFTI could be detected however masses for the C-terminal truncated peptides –PD (1291.6 m/z) and –FPD (1172.6 m/z) were observed.

**a**

```
p15_OaAEP1b       1 MHHHHHHHHLVPRGSARDGDYLHLPSEVSRFFRPQETNDDHGEDSVGTRWAVLIAGSKGYANYRHQAGVCHAYQILKRGG  80
P15_OaAEP1b_MLA   1 MHHHHHHHHLVPRGSARDGDYLHLPSEVSRFFRPQETNDDHGEDSVGTRWAVLIAGSKGYANYRHQAGVCHAYQILKRGG  80
                    ********************************************************************************

p15_OaAEP1b      81 LKDENIVVFMYDDIAYNESNPRPGVIINSPHGSDVYAGVPKDYTGEEVNAKNFLAAILGNKSAITGGSGKVVDSGPNDHI 160
P15_OaAEP1b_MLA  81 LKDENIVVFMYDDIAYNESNPRPGVIINSPHGSDVYAGVPKDYTGEEVNAKNFLAAILGNKSAITGGSGKVVDSGPNDHI 160
                    ********************************************************************************

p15_OaAEP1b     161 FIYYTDHGAAGVIGMPSKPYLYADELNDALKKKHASGTYKSLVFYLEACESGSMFEGILPEDLNIYALTSTNTTESSWCY 240
P15_OaAEP1b_MLA 161 FIYYTDHGAAGVIGMPSKPYLYADELNDALKKKHASGTYKSLVFYLEACESGSMFEGILPEDLNIYALTSTNTTESSWCY 240
                    ********************************************************************************

p15_OaAEP1b     241 YCPAQENPPPPEYNVCLGDLFSVAWLEDSDVQNSWYETLNQQYHHVDKRIS-----HASHATQYGNLKLGEEGLFVYMGS 315
P15_OaAEP1b_MLA 241 YCPAQENPPPPEYNVCLGDLFSVAWLEDSDVQNSWYETLNQQYHLVKARTSNGNSAYASHATQYGNLKLGEEGLFVYMGS 320
                    ****************************************** *  * *      ************************

p15_OaAEP1b     316 NPANDNYTSLDGNALTPSSIVVNQRDADLLHLWEKFRKAPEGSARKEVAQTQIFKAMSHRVHIDSSIKLIGKLLFGIEKC 395
P15_OaAEP1b_MLA 321 NPANDNYTSLDGNALTPSSIVVNQRDADLLHLWEKFRKAPEGSARKEEAQTQIFKAMSHRVHIDSSIKLIGKLLFGIEKC 400
                    ********************************************** ******************************

p15_OaAEP1b     396 TEILNAVRPAGQPLVDDWACLRSLVGTFETHCGSLSEYGMRHTRTIANICNAGISEEQMAEAASQACASIP* 467
P15_OaAEP1b_MLA 401 TEILNAVRPAGQPLVDDWACLRSLVGTFETHCGSLSEYGMRHTRTIANICNAGISEEQMAEAASQACASIP  471
                    ************************************************************************
```

.

**b**

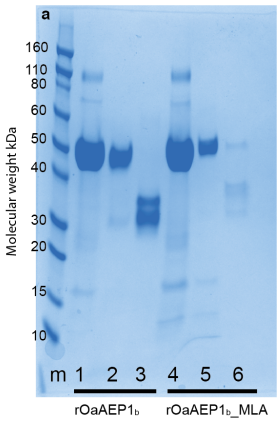


**Supplementary Figure 7. Recombinant production of OaAEP1$_b$ and OaAEP1$_b$_MLA. a**, The OaAEP1$_b$ and OaAEP1$_b$_MLA fusion protein sequences. For each, the putative signal peptide regions were removed and replaced with eight Histidine's allowing the capture of inactivated enzyme. **b**, Imidiazole at 250mM was used to elute rOaAEP1b and rOaAEP1b_MLA zymogens (lanes 1 and 4 respectively). AEP zymogens were self-activated at pH4.5 for 4 hours at 37°C followed by an overnight incubation at 4°C. Under these conditions activation appeared not complete (lanes 2 and 5) but was sufficient to enable purification of active enzyme by cation exchange chromatography (lanes 3 and 6).

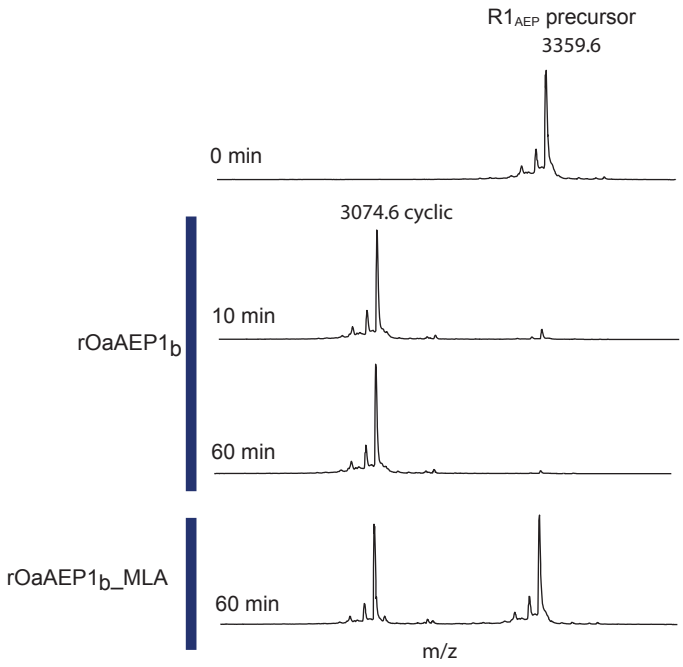


**Supplementary Figure 8.** ***In vitro*** **assessment of rOaAEP1b and rOaAEP1b_MLA activity on the model peptide R1. a**, Representative MALDI MS spectra of the $R1_{AEP}$ precursor peptide following incubation with recombinant $OaAEP1_b$ and $OaAEP1_b$_MLA (23.5 µg $mL^{-1}$ total protein). For rOaAEP1b, all precursor peptide was converted to cyclic R1 (3074.6 m/z) within ten minutes, while substantial precursor peptide remained in the case of $OaAEP1_b$_MLA even after 60 minutes incubation. Observed monoisotopic masses (Da; $[M+H]^+$) are listed.

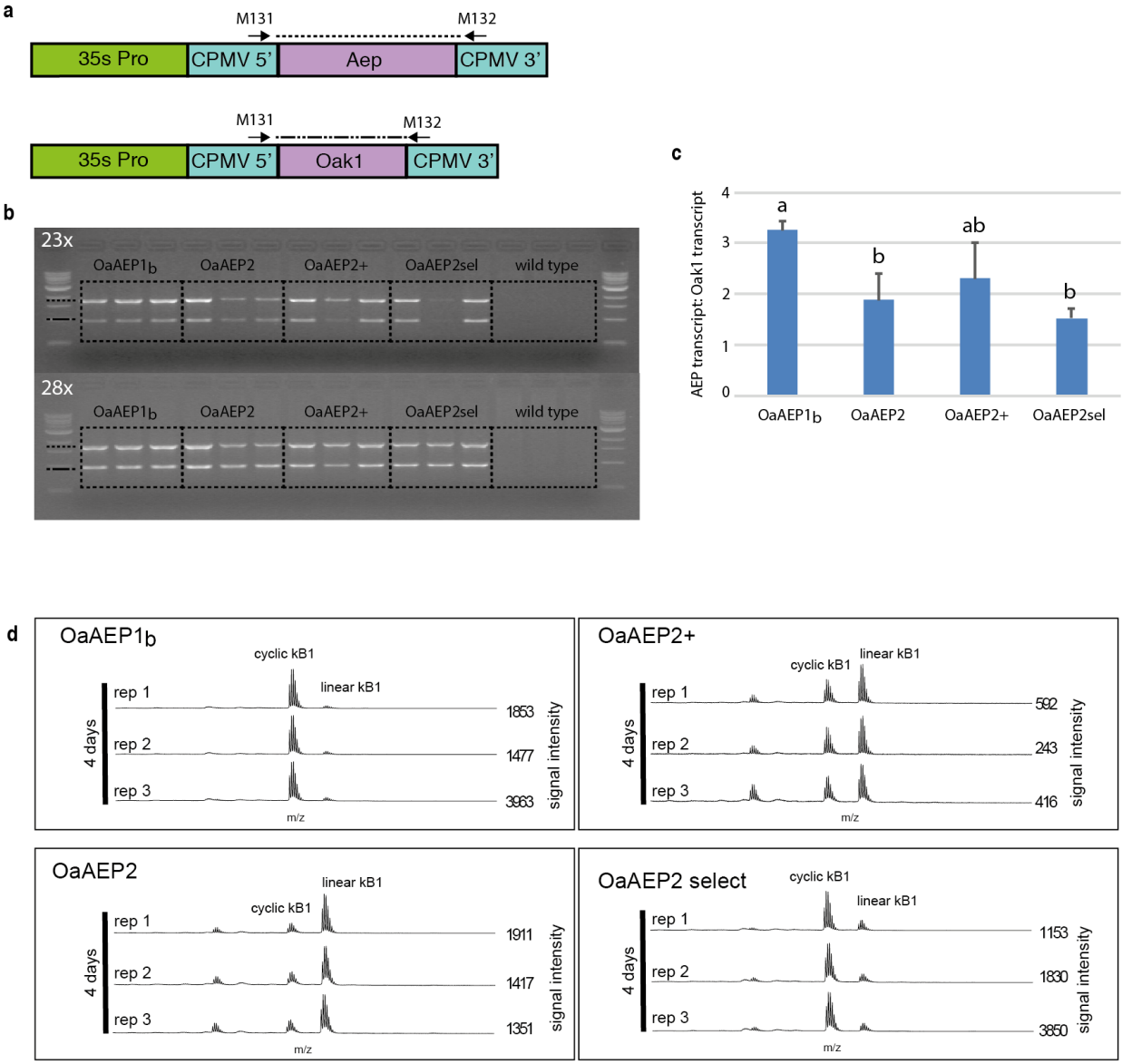


**Supplementary Figure 9. AEP transgene expression levels are consistent despite significant differences in Oak1 processing. a**, Plant AEP genes and *oak1* were engineered for *in planta* expression by insertion into the pEAQ-Dest1 vector [10] which contains the 35s promoter and Cowpea mosaic virus (CPMV) 5' and 3' UTR sequences. For the *N. benthamiana* leaf infiltrations, the density of Agrobacterium containing the pEAQ-Oak1 expression vector was kept constant irrespective of the co-expressed AEP. This allows an assessment of AEP transcript levels by normalizing to *Oak1* transcript. **b,** PCR analysis of *Oak1* transcript abundance (lower band) compared to AEP transcript (upper band) at PCR cycle 23 and 28 respectively. Primers M131 (5'-GACGAGGTATTGTTGCCTG-3') and M132 (5'-CCGCTCACCAAACATAG-3') were designed to bind within the 5' and 3' UTR respectively. **c,** Transcript densitometry analysis reveals a slight increase in transcript for OaAEP1$_b$, but similar levels for OaAEP2 and OaAEP2 engineered variants (OaAEP2+ and OaAEP2select) n=3. **d,** Peptide analysis at 4 days post-infiltration (n=3).

**Supplementary Figure 10. Alignment of *Gossypium raimondii* AEP sequences.** Protein sequences were aligned using ClustalW[6]. Identical residues are marked with a star and similar residues with a dot. Putative signal peptides predicted by SignalP 4.0[7] are italicized with putative propeptide cleavage sites indicated by arrows and proposed based on[8]. Boxed residues indicate putative N-terminal vacuole targeting signals as predicted by[9]. The catalytic histidine and cysteine residues are bolded. The residue homologous to the gatekeeper residue of OaAEP1$_b$ [8] is shown in green with the cysteine flanking poly-proline loop in blue. The marker of ligase activity (MLA) (this study) is shown in magenta. Underlined are residues in homologous positions to those predicted by the protein space modelling as important for ligase function (Fig. 4c).


**Supplementary Figure 11. Alignment of *Hybanthus enneaspermus* AEP sequences.** Protein sequences were aligned using ClustalW[6]. Identical residues are marked with a star and similar residues with a dot. Putative signal peptides predicted by SignalP 4.0[7] are italicized with putative propeptide cleavage sites indicated by arrows and proposed based on [8]. Boxed residues indicate putative N-terminal vacuole targeting signals as predicted by[9]. The catalytic histidine and cysteine residues are bolded. The residue homologous to the gatekeeper residue of OaAEP1$_b$[8] is shown in green with the cysteine flanking poly-proline loop in blue. The marker of ligase activity (MLA) (this study) is shown in magenta. Underlined are residues in homologous positions to those predicted by the protein space modelling as important for ligase function (Fig. 4c).

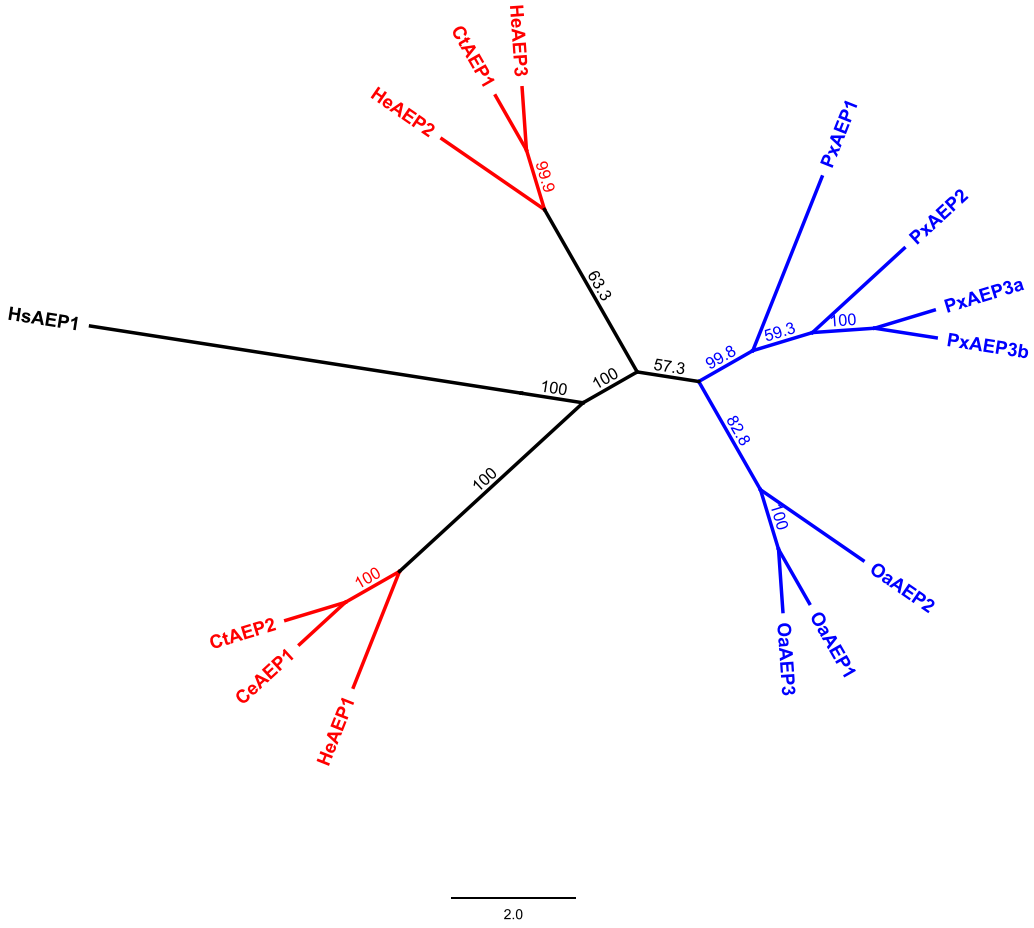


**Supplementary Figure 12. Phylogentic tree of plant AEPs which differ in functional preference.** AEPs are grouped into two broad groups the Asterids (red text) vs Rosids (blue text). Ligase-type and protease type AEPs are intermixed in the respective clades, especially in the Asterids (includes the Rubiaceae and Solanaceae). Ligase-type AEPs are not more closely related to one another but share greatest homology with intra-specific AEPs. The tree is rooted with human AEP (HsAEP1) and is a consensus neighbor-joining tree of 1000 bootstrapped trees.

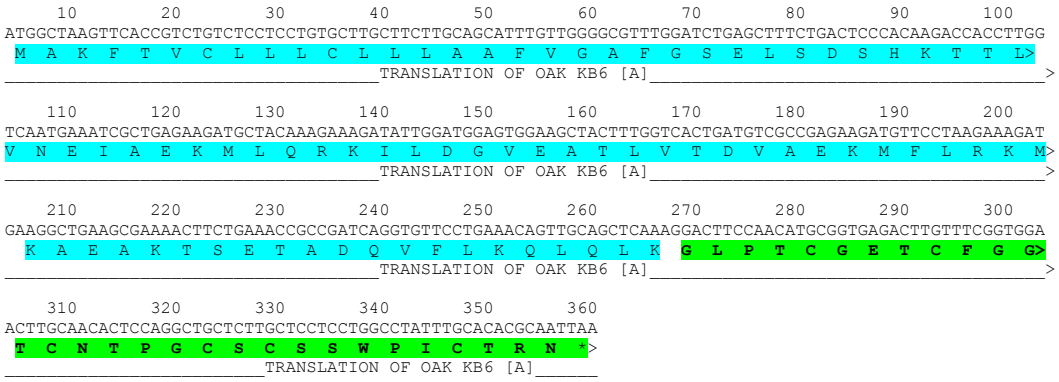


**Supplementary Figure 13.** DNA and protein sequence of *Oak1-kB6trunc*.

**Supplementary Table 1**. RNA-seq summary statistics

| RNA-seq Summary Statistics | | |
|---|---|---|
| | ***Hybanthus enneaspermus*** | ***Petunia* x *hybrida* 'Mitchell'** |
| **SRA accession codes** | SRP127205 | SRP127205 |
| **Pre-QC** | | |
| Number of sequences | 217735426 | 87112662 |
| Sequence length | 100 | 150 |
| Mean PHRED score | Q36 | Q37 |
| **Post-QC** | | |
| Number of sequences | 217335174 | 87112662 |
| Sequence length | 90 | 131 |
| Mean PHRED score | Q37 | Q37 |
| Percent of bases passing QC | 89.8% | 87.3% |
| **Assembly Statistics** | | |
| Assembly name | HennT2.1 | Px_ReTri2 |
| Total number of bases assembled | 124228394 | 80647009 |
| Total number of transcripts | 113823 | 163860 |
| Total number of putative genes | 85016 | 129686 |
| Mean transcript length | 1091.42 | 713.26 |

**Supplementary Table 2. Functionally verified ligase and protease-type AEPs used for the protein space modelling.**

| | | *Reference* |
|---|---|---|
| ***Ligases*** | *Oldenlandia affinis* OaAEP1 (KR259377) | *11* |
| | *Oldenlandia affinis* OaAEP1$_b$ (KR259377 with 9A-G and 1112A-T) | *12, current study* |
| | *Oldenlandia affinis* OaAEP3 (KR259378) | *12, current study* |
| | *Oldenlandia affinis* OaAEP4_.173926. | *12, current study* |
| | *Clitoria ternatea* Butelase-1 (KF918345) | *current study* |
| | *Petunia hybrida* PxAEP3b (MG720076) | *12, current study* |
| ***Proteases*** | *Oldenlandia affinis* OaAEP2 (KR259378) | *12, current study* |
| | *Clitoria ternatea* CtAEP2 (butelase-2) (KR912009) | *12* |
| | *Clitoria ternatea* CtAEP6 (KY640209) | *current study* |
| | *Petunia hybrida* PxAEP1 (MG720071) | *current study* |
| | *Petunia hybrida* PxAEP2 (MG720075) | *current study* |
| | *Petunia hybrida* PxAEP3a (MG720072) | *13* |
| | *Arabidopsis thaliana* _delta (AEE76347.1) | *13* |
| | *Arabidopsis thaliana* _gamma (BAA18924.1) | *13* |
| | *Arabidopsis thaliana* _alpha (AEC07775.1) | *13* |
| | *Arabidopsis thaliana* _beta (BAA09615.1) | *13* |
| | *Nicotiana benthamiana*_AEP1a (BAD51740.1) | *13* |
| | *Nicotiana benthamiana*_AEP1b (BAD51741.1) | |

**Supplementary Table 3. Predictive residues for AEP ligase activity.** $Resn_{(MSA)}$ = residue column number in alignment, $Resn_{(ppOaAEP1)}$ = residue number in ppOaAEP1, DISORD = disorder propensity, CHRG = net static charge, RMW = molecular weight of R group, HPATH = hydropathy index.


| $Resn_{(MSA)}$ | $Resn_{(ppOaAEP1)}$ | Property | Load | PC | Ligase | Protease |
|---|---|---|---|---|---|---|
| **180** | **139** | CHRG | -0.18 | 6 | K | D |
| **180** | **139** | CHRG | 0.22 | 7 | K | D |
| **219** | **161** | CHRG | -0.07 | 5 | D | N |
| **274** | **186** | CHRG | 0.18 | 7 | K | G |
| **280** | **192** | CHRG | -0.18 | 5 | D | N |
| **280** | **192** | CHRG | -0.16 | 7 | D | N |
| **352** | **247** | RMW | 0.07 | 7 | C | G |
| **353** | **248** | RMW | 0.10 | 7 | Y | T |
| **359** | **253** | CHRG | 0.10 | 5 | Q | E |
| **359** | **253** | CHRG | 0.08 | 7 | Q | E |
| **361** | **255** | DISORD | -0.13 | 5 | A | P |
| **379** | **263** | HPATH | 0.08 | 5 | V | T |
| **379** | **263** | HPATH | 0.07 | 7 | V | T |
| **506** | **293** | HPATH | 0.21 | 6 | H | L |
| **506** | **293** | RMW | -0.10 | 6 | H | L |
| **506** | **293** | CHRG | -0.10 | 6 | H | L |
| **506** | **293** | DISORD | -0.08 | 6 | H | L |
| **506** | **293** | CHRG | -0.12 | 7 | H | L |
| **506** | **293** | HPATH | 0.08 | 7 | H | L |
| **519** | **n/a** | NOTGAP | 0.13 | 6 | - | N |
| **519** | **n/a** | NOTGAP | -0.08 | 7 | - | N |
| **520** | **n/a** | CHRG | 0.07 | 5 | - | G |
| **520** | **n/a** | NOTGAP | 0.13 | 6 | - | G |
| **520** | **n/a** | NOTGAP | -0.08 | 7 | - | G |
| **521** | **n/a** | HPATH | 0.08 | 5 | - | N |
| **521** | **n/a** | NOTGAP | 0.10 | 6 | - | N |
| **521** | **n/a** | NOTGAP | -0.10 | 7 | - | N |
| **521** | **n/a** | RMW | 0.09 | 7 | - | N |
| **526** | **n/a** | NOTGAP | 0.13 | 6 | - | S |
| **542** | **314** | CHRG | -0.19 | 5 | E | K |
| **542** | **314** | HPATH | 0.07 | 5 | E | K |
| **542** | **314** | DISORD | -0.07 | 5 | E | K |
| **544** | **316** | RMW | -0.13 | 5 | G | K |
| **544** | **316** | DISORD | 0.09 | 5 | G | K |
| **544** | **316** | CHRG | -0.07 | 7 | G | K |

**Supplementary Table 4.** AEP sequences retrieved from public sequence databases that contain either a minimal MLA region or hydrophobic patch (GRAVY score > 0). Underlined are potential N-glycosylation sites and in brackets are GRAVY scores). In bold is the Gatekeeper residue homologous to Cys247 in $OaAEP1_b$.

| Plant species | Accession | MLA (GRAVY) | Gate Keeper | Putative ligase |
|---|---|---|---|---|
| *Punica Granatum* | OWM76945.1 | RTNASH | NSW**G**CY | no |
| *Helianthus annuus* | OTG32548.1 | RIAIDKVTGFGSH (0.3) | NSW**A**TY | yes |
| | OTG32550.1 | RIAIDKVTGFGSH (0.3) | NSW**A**TY | yes |
| *Spinacia oleracea* | KNA12580.1 | RTSRMSH | SSY**A**TY | yes |
| *Beta Vulgaris* | XP_010669190.1 | RTSKLSH | SSY**A**TY | yes |
| | KMT17971.1 | RTSKLSH | SSY**A**TY | yes |
| *Daucus carota* | XP_017221562.1 | RTSNDSH | DSW**A**TY | no |
| | KZM84774.1 | RTSNDSH | DSW**A**TY | no |
| | KZM84775.1 | RASNYSH | NSW**A**TY | no |
| | XP_017221563.1 | RASNYSH | NSW**A**TY | no |
| | KZM84773.1 | RTSNYSH | DSW**A**TY | no |
| | XP_017221560.1 | RTSNYSH | DSW**A**TY | no |
| *Eucalyptus grandis* | XP_010034096.1 | RTNMSH | SSY**G**YY | no |
| *Theobroma cacao* | EOY26259.1 | RTAVDNLVVSSH (0.4) | NSW**G**TY | no |
| *Gossypium raimondii* | Gorai.009G046800.1 | RATTSH | SSW**A**TY | yes |
| *Malus domestica* | MDP0000937205 | RTNKSH | SSY**G**TY | no |

**Supplementary Table 5. Predictive power of the 16 most ligase-predictive residues.** Known ligases are in red, and known proteases are in blue. A score of 100% would indicate that all 16 predictive residues are an identical match in the AEP sequence.

| | |
|---|---|
| *Oldenlandia affinis* OaAEP1 (KR259377) | 94% |
| *Oldenlandia affinis* OaAEP1$_b$ (KR259377 with 9A-G and 1112A-T) | 94% |
| *Oldenlandia affinis* OaAEP3 (KR259378) | 88% |
| *Oldenlandia affinis* OaAEP_4_.173926. | 88% |
| *Clitoria ternatea* Butelase-1 (KF918345) | 25% |
| *Hybanthus enneaspermus* HeAEP-3 (MG720074) | 44% |
| *Petunia hybrida* PxAEP3b (MG720076) | 38% |
| *Oldenlandia affinis* OaAEP2 (KR259378) | 13% |
| *Clitoria ternatea* Butelase-2) (KR912009) | 0% |
| *Clitoria ternatea* CtAEP6 (KY640209) | 38% |
| *Petunia hybrida* PxAEP1 (MG720071) | 0% |
| *Petunia hybrida* PxAEP2 (MG720075) | 6% |
| *Petunia hybrida* PxAEP3a (MG720072) | 6% |
| *Hybanthus enneaspermus* HeAEP-1 (MG720073) | 6% |
| *Hybanthus enneaspermus* HeAEP-2 (MG720070) | 13% |
| *Arabidopsis thaliana* _delta (AEE76347.1) | 0% |
| *Arabidopsis thaliana* _gamma (BAA18924.1) | 6% |
| *Arabidopsis thaliana* _alpha (AEC07775.1) | 6% |
| *Arabidopsis thaliana* _beta (BAA09615.1) | 0% |
| *Nicotiana benthamiana*_AEP1a (BAD51740.1) | 6% |
| *Nicotiana benthamiana*_AEP1b (BAD51741.1) | 0% |

**Supplementary Table 6.** Preferred ligase residue identities for all functionally assigned AEPs with ligase prediction scores of 25% or above. Known ligases are in red, and known proteases are in blue. Predictive residues listed on the right (red if ligase predictive residue present, otherwise white). The numbering is given relative to the OaAEP1$_b$ with the Gatekeeper residue shown in green, polyproline loop residues in blue and MLA residues in magenta.

| | **Resn$_{(ppOaAEP1)}$** | **139** | **161** | **186** | **192** | **247** | **248** | **253** | **255** | **263** | **293** | **n/a** | **n/a** | **n/a** | **n/a** | **314** | **316** |
|---|---|---|---|---|---|---|---|---|---|---|---|---|---|---|---|---|---|
| OaAEP1 (KR259377) | 94% | 1 | 1 | 1 | 1 | 1 | 1 | 1 | 0 | 1 | 1 | 1 | 1 | 1 | 1 | 1 | 1 |
| OaAEP1b* | 94% | 1 | 1 | 1 | 1 | 1 | 1 | 1 | 0 | 1 | 1 | 1 | 1 | 1 | 1 | 1 | 1 |
| OaAEP3 (KR259378) | 88% | 1 | 1 | 1 | 1 | 1 | 1 | 1 | 1 | 1 | 0 | 1 | 1 | 1 | 1 | 0 | 1 |
| OaAEP4 | 88% | 1 | 1 | 1 | 1 | 1 | 1 | 1 | 1 | 1 | 0 | 1 | 1 | 1 | 1 | 0 | 1 |
| Butelase-1 (KF918345) | 25% | 0 | 1 | 1 | 0 | 0 | 0 | 1 | 0 | 1 | 0 | 0 | 0 | 0 | 0 | 0 | 0 |
| HeAEP-3 (MG720074) | 44% | 0 | 1 | 1 | 0 | 0 | 0 | 0 | 0 | 1 | 0 | 1 | 1 | 1 | 1 | 0 | 0 |
| PxAEP3b (MG720076) | 38% | 0 | 1 | 1 | 0 | 0 | 0 | 1 | 0 | 0 | 0 | 1 | 1 | 1 | 0 | 0 | 0 |
| CtAEP6 (KY640209) | 38% | 0 | 0 | 0 | 1 | 0 | 0 | 0 | 1 | 0 | 0 | 1 | 1 | 1 | 1 | 0 | 0 |

*KR259377 with substitutions 9A-G and 1112A-T to produce OaAEP1$_b$

**Supplementary References**


1 Poth, A. G., Colgrave, M. L., Lyons, R. E., Daly, N. L. & Craik, D. J. Discovery of an unusual biosynthetic origin for circular proteins in legumes. *Proc. Natl. Acad. Sci. U. S. A.* **108**, 10127-10132 (2011).

2 Poth, A. G. *et al.* Discovery of Cyclotides in the Fabaceae Plant Family Provides New Insights into the Cyclization, Evolution, and Distribution of Circular Proteins. *ACS Chem. Biol.* **6**, 345-355 (2011).

3 Rosengren, K. J., Daly, N. L., Plan, M. R., Waine, C. & Craik, D. J. Twists, knots, and rings in proteins - Structural definition of the cyclotide framework. *J. Biol. Chem.* **278**, 8606-8616 (2003).

4 Tank, D. C. *et al.* Nested radiations and the pulse of angiosperm diversification: increased diversification rates often follow whole genome duplications. *New Phytol.* **207**, 454-467 (2015).

5 Poth, A. G. *et al.* Cyclotides associate with leaf vasculature and are the products of a novel precursor in *Petunia* (Solanaceae). *J. Biol. Chem.* **287**, 27033-27046 (2012).

6 Larkin, M. A. *et al.* Clustal W and Clustal X version 2.0. *Bioinformatics* **23**, 2947-2948 (2007).

7 Petersen, T. N., Brunak, S., von Heijne, G. & Nielsen, H. SignalP 4.0: discriminating signal peptides from transmembrane regions. *Nat. Methods* **8**, 785-786 (2011).

8 Yang, R. L. *et al.* Engineering a Catalytically Efficient Recombinant Protein Ligase. *J. Am. Chem. Soc.* **139**, 5351-5358 (2017).

9 Jackson, M. A. *et al.* A bioinformatic approach to the identification of a conserved domain in a sugarcane legumain that directs GFP to the lytic vacuole. *Functional Plant Biology* **34**, 633-644 (2007).

10 Sainsbury, F., Thuenemann, E. C. & Lomonossoff, G. P. pEAQ: versatile expression vectors for easy and quick transient expression of heterologous proteins in plants. *Plant Biotechnol. J.* **7**, 682-693 (2009).

11 Harris, K. S. *et al.* Efficient backbone cyclization of linear peptides by a recombinant asparaginyl endopeptidase. *Nat. Commun.* **6**, 10199 (2015).

12 Poon, S. *et al.* Co-expression of a cyclizing asparaginyl endopeptidase enables efficient production of cyclic peptides in planta. *J. Exp. Bot.* **69**, 633-641 (2017).

13 Gillon, A. D. *et al.* Biosynthesis of circular proteins in plants. *Plant J.* **53**, 505-515 (2008).